Macromolecular Research, Vol. 20, No. 1, pp 84-92 (2012)
DOI 10.1007/s13233-012-0002-9
www.springer.com/13233

Polyaniline Nanofiber-Coated Polystyrene/Graphene Oxide Core-Shell Microsphere Composites

Ali Grinou, Young Soo Yun, and Hyoung-Joon Jin*

Department of Polymer Science and Engineering, Inha University, Incheon 402-751, Korea

Received May 26, 2011; Revised July 18, 2011; Accepted July 19, 2011

Abstract: A simple method was used to synthesize the polyaniline nanofiber-coated polystyrene/graphene oxide (PANI-PS/GO) core shell composite using a solution mixing process. GO could be easily coated on PANI-coated PS to form a PANI-PS/GO core shell structure through the ring-opening reaction of the epoxide groups in the GO sheets with amine groups in the PANI nanofibers. The existence of PANI in the PS and PS/GO core shell composite was confirmed by the appearance of a new peak in the photoelectron spectroscopy and energy-dispersive X-ray spectroscopy results assigned to the nitrogen band. Thermal investigation showed that the addition of GO to the PANI-coated PS increased the glass transition temperature of the PANI-PS/GO composites. The thermal stability of the composites was also improved compared to that of neat PS. Electrical conductivity investigation using a four-probe resistivity measurement system showed that PANI addition to the composite not only enhanced the interfacial interaction but also improved the electrical conductivity of the composite. The increased electrical conductivity of the final composite may enable potential electronic applications.

Keywords: nano composites, polymer-matrix composites (PMCs), thermal properties, photoelectron spectroscopy (XPS), transmission electron microscopy (TEM).

Introduction

Nanocarbon materials, such as carbon nanotubes (CNT) and graphene nanosheets (GNS), have been studied extensively as one of the most exciting materials for electronic applications owing to their remarkable properties.[1,2] In particular, the high aspect ratio combined with exceptional conductivity make GNS a promising choice as a conducting filler in polymers that is comparable to that of CNT.[3] This GNS can be synthesized through the simple chemical reduction of graphene oxide (GO).[4] GO sheets can be synthesized through the oxidative treatment of graphite.[5] The resulting GO is made up of hydrophilic oxygenated graphene sheets, whose basal planes are coated mostly with epoxide, hydroxyl, carbonyl, and carboxyl groups.[6,7] Owing to their hydrophilic nature, GO sheets are readily dispersed in water as individual sheets.[8,9] The high dispersion stability of GO has attracted interest in applications as nanoelectronic and functional nanocomposites materials.[10] Considerable effort has been made to incorporate GO into polymer composites with superior properties, such as high mechanical strength and flexibility.[11] These materials can produce a new type of material that combines the properties of GO with the structural properties of the polymer.[12]

Recently, a range of polymer microspheres/GO nanocomposites has been synthesized, such as polymethylmethacrylate/GO nanocomposites[13] and polystyrene/GO (PS/GO) composites.[14] These microspheres coated with GO composites have many applications, such as electrically conducting particles for electrorheological fluids[15] and GO hollow spheres[16] that are fabricated by removing the polymer particles from the GO/polymer microsphere. The interfacial interaction between GO and polymer matrix is a crucial factor to improve the properties of the polymer composites. Therefore, different strategies have been used to increase the interfacial interaction between GO and the polymer matrix, such as using surfactants[17] and the covalent functionalization of GO,[18] in order to attach the organic groups to the surface of the GO grafted with the polymer matrix to obtain a uniform and stable dispersion of GO in the polymer matrix. A homogenous dispersion and good interfacial interaction strongly enhance the proprieties of the composite.

The nanocomposites prepared by solution mixing process exhibit higher compatibility at the interface. In addition, the mechanical properties increase when the nanocomposite is synthesized by the solution mixing method. Moreover, the glass transition temperature (T_g) is raised by the addition of the filler. These results imply the presence of a strong adhesion at the filler/polymer interface, in particular, in the case of the composite synthesized by the solution mixing process

*Corresponding Author. E-mail: hjjin@inha.ac.kr

compared to other methods.[19] They also suggest that a more intensive intercalation is obtained at the interface due to the solution mixing process. This method is considered as effective measure to prepare composites with a homogenous nanocarbon materials distribution into the polymer matrix and is often used to prepare composite films.[20]

In this study, a rapid mixing polymerization method was used to incorporate polyaniline (PANI) nanofibers onto the surface of sulfonated PS (s-PS) microspheres. In this simple method, GO sheets can be easily coated on the PANI-coated PS to form a PANI-PS/GO core-shell structure through a ring opening reaction of the epoxide groups in the GO sheets with the amine groups in the PANI nanofibers. The strong adhesion of the GO sheets on the PS achieved via the intermediary layer of PANI nanofibers was attributed to the good interfacial interaction between GO and PS through the interaction of amine groups in PANI and epoxide groups in GO. In addition, the PANI nanofibers not only enhance the interfacial interaction, but also improve the electrical conductivity of the composite.

Experimental

Materials. GO was synthesized from graphite flakes purchased from Sigma-Aldrich (Product Number 332461). Styrene monomer (Kanto Chemical, Japan) was washed five times with a 10 mol% aqueous solution of sodium hydroxide (NaOH) and stored in a refrigerator. Polyvinylpyrrolidone (PVP, Mw=55,000 g/mol, Aldrich) was used as a stabilizer without purification. 2,2-Azobisisobutyronitrile (AIBN, JUNSEI, Japan) was used as an initiator and was dissolved in ethanol to remove the inhibitor, which was precipitated at -4 °C, then stored in a refrigerator prior to polymerization. The aniline monomer was purchased from DC Chemical Co. Ltd. (Korea). Ammonium persulfate (APS, 98%) was purchased from Daejung Chemicals and Materials Co. Ltd. (Korea). Sulfuric acid (H_2SO_4), sodium nitrate ($NaNO_3$), potassium permanganate ($KMnO_4$) and all other organic solvents used in this study were used as received.

Preparation of Graphene Oxide (GO). The GO was synthesized using the Hummers method.[5] Briefly, 70 mL of concentrated sulfuric acid (H_2SO_4) was transferred into a 250 mL round bottom flask. Sodium nitrate ($NaNO_3$, 0.5 g), was then added to the sulfuric acid and stirred for 5 min. Graphite flakes (1 g) were added to the solution with 5 min stirring. $KMnO_4$ (3 g) was added gradually to the dark mixture, and the reaction mixture was stirred at room temperature for 30 min. The solution was transferred to a 70 mL vial, sonicated for 15 min and stirred continuously for 3 h. The solution was added slowly to 600 mL of deionized (DI) water and 34% hydrogen peroxide (300 mL) was added immediately. The reaction mixture was then stirred for 5 min, filtered and washed several times with DI water until pH=7. The black powder was added to 70 mL of DI water and sonicated for 4 h, followed by three periods of centrifugation. The solution was filtered again to leave a brown residue, indicating the successful oxidation of graphite. The solution was dried under a vacuum at 60 °C for three days.

Preparation of Polystyrene (PS) Microspheres *via* Suspension Polymerization. Suspension polymerization was carried out in a 250 mL bottom flask at 70 °C for 12 h. PVP (1.5 wt%) was dissolved in DI water and poured into the reactor. The styrene monomer and AIBN were added to the reactor, and the mixture solution was then homogenized at 960 rpm using an Ultra-Turrax T 25 (Ika Labortechnik, Staufen, Germany) to form stable microspheres. The polymerization products were rinsed with ethanol and centrifuged repeatedly to remove the unreacted styrene monomer and PVP. The PS microspheres were then dried in a vacuum oven at room temperature for 48 h.

Sulfonation of Polystyrene (s-PS). Sulfonated PS was synthesized using the procedure described previously.[21] Briefly, 50 mL of concentrated sulfuric acid (H_2SO_4) was transferred to a 100 mL round bottom flask. The dried PS powder (200 mg) was then added to the H_2SO_4 and sonicated for 1 h. After ultrasonic dispersion, sulfonation was allowed to take place at 40 °C with magnetic stirring for 24 h. When cooled to room temperature, the product was separated by repeated centrifugation (6,000 rpm) and washed with a large excess of ethanol. Finally, a yellow powder was obtained after being dried.

Preparation of Polyaniline Nanofiber-Coated PS (PANI-PS). Sulfonated PS powder (200 mg) was dispersed in 20 mL of DI water, to which 20 mg of aniline monomer in 5 mL of a 3 M HCl solution was added. The mixture was stirred for 4 h at room temperature, after which 40 mg of APS was dissolved in 10 mL 3 M HCl and added rapidly to the s-PS/aniline monomer mixture to start the polymerization of aniline on the s-PS surface. The reaction mixture was stirred with a magnetic bar for 12 h at room temperature to ensure complete polymerization. The green powder was filtered and rinsed several times with ethanol. Finally, the powder was dried under vacuum at 50 °C for 24 h.

Synthesis of PANI-PS/GO Core-Shell Microsphere Composite. Homogenous composites of PANI-coated PS and GO were prepared by a solution mixing process. Briefly, 300 mg of PANI-coated PS was dissolved in 100 mL of ethanol with magnetic stirring for 4 h. GO powder (20 mg) was dispersed in 20 mL of DI water and sonicated for 2 h to obtain a homogeneous solution. After ultrasonic dispersion, the GO solution was added to the above solution of PANI-PS and treated ultrasonically for 4 h to ensure a uniformly dispersion of GO on the surface of the PANI-coated PS. The mixture was stirred for an additional 12 h at room temperature to ensure complete reaction. The product was filtered, rinsed several times with ethanol, and dried under vacuum at 50 °C for 24 h.

Extraction of PS from the PANI-PS and PANI-PS/GO Core-Shell Microsphere Composite. Ten milligrams of

PANI-coated PS was dispersed in 5 mL of tetrahydrofuran (THF) and stirred for 24 h to ensure complete reaction. Finally, the resulting product was filtered, washed three times with THF and DI water. The black residue was dried under vacuum at 50 ºC for 24 h. The same procedure was used for the PANI-PS/GO core-shell microsphere composite, to confirm the existence of PANI and GO after the extraction of PS from the composite.

Measurements and Characterization. After pre-coating the sample with a homogeneous Pt layer by ion sputtering (E-1030, Hitachi, Japan), the morphology of the microspheres was observed by field emission scanning electron microscopy (FESEM, S-4200, Hitachi, Japan) at an accelerating voltage of 15 kV. The existence of PANI and GO incorporated in the PS microspheres was confirmed by transmission electron microscopy (TEM, CM200, Philips, USA) at an accelerating voltage of 100 kV. The TEM samples were prepared by dispersing a small amount of the dry powder in ethanol and placing a drop on the grid. FTIR, photoelectron spectroscopy (XPS) and FT-Raman spectroscopy were used to characterize the chemical structures of the neat PS, PANI, PANI-PS, and PANI-PS/GO core-shell composites. The samples underwent thermal analysis using a Perkin-Elmer differential scanning calorimeter (DSC) under a continuous nitrogen flow. All specimens were weighed in the range of 4-5 mg and were examined between room temperature and 260 ºC at a scanning rate of 20 ºC/min. Thermogravimetric analysis (TGA, TA instruments, Q50, UK) was used to measure the thermal stability of the neat PS, neat PANI, GO, PANI-PS and PANI-PS/GO core-shell composites. TGA was carried out at a heating rate of 10 ºC/min from 20 to 730 ºC under a dynamic nitrogen flow of 10 cm^3/min. The electrical conductivity of the neat PANI, PANI-PS and PANI-PS/GO core-shell composites was measured using a four-probe method with an electrical conductivity meter (Hiresta-UP MCP-HT450, Mitsubishi Chemical, Japan). The samples were prepared in the form of disc-type pellets with a thickness of 0.5 mm using a press at room temperature at an applied pressing force of 1 ton.

Results and Discussion

Figure 1 shows the FTIR spectra of (a) PS, (b) PANI, (c) PANI-PS, (d) PANI-PS/GO, and (e) GO. Typical PS absorption bands at 3027, 2920, 1593, 1497, 704, and 527 cm^{-1} are clearly evident in the pure PS in Figure 1(a). These peaks were attributed to the characteristic aromatic =C-H, -CH_2-, aromatic C=C, and monosubstituted ring.[22] For the pure PANI nanofiber of Figure 1(b), the bands at 1561 and 1465 cm^{-1} show the characteristic C=C stretching vibrations of the quinoid and benzenoid rings, respectively, indicating the oxidized polyaniline state of the emeraldine salt. The 1303 and 1239 cm^{-1} bands were assigned to the bending vibrations of N-H and the asymmetric C-N stretching modes of

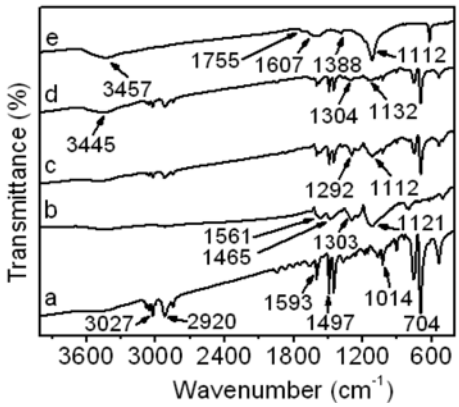

Figure 1. FTIR spectra of (a) pure PS, (b) pure PANI, (c) PANI-PS, (d) PANI-PS/GO composite, and (e) GO.

the polaron structure of PANI, respectively.[23] The strong band at 1121 cm^{-1} is a characteristic of the electronic-like band described by Mac Diarmid *et al*.,[24] which is a measure of the degree of delocalization of electrons and thus a characteristic peak of PANI conductivity. For the PANI-PS shown in Figure 1(c), both PS and PANI peaks are shown in the PANI-PS spectrum, which confirmed the existence of PANI on the surface of the PS microspheres. For the PANI-PS/GO of Figure 1(d), a new peak appeared at 3445 cm^{-1} corresponding to the OH band of GO, and the slight shift in the wavenumbers of the N-H band of PANI indicated the successful interaction of GO with PANI on the PS surface. The spectrum of GO in Figure 1(e) shows a broad band at 3457 cm^{-1}, which was assigned to OH groups, and the bands at 1755 and 1607 cm^{-1} were assigned to carboxyl and carbonyl groups. Other peaks, such as C-OH (1388 cm^{-1}) and C-O-C (1112 cm^{-1}), correspond to the C-O functionalities.[25] These main characteristic peaks indicated that GO had been synthesized successfully.

The existence of PANI in the PANI-PS and PANI-PS/GO core-shell composite was confirmed by the appearance of a new peak at 399.6 eV, which was assigned to the nitrogen band (N1s) of PANI using XPS characterization, as shown in Figure 2, indicating the successful polymerization of aniline on the surface of the PS microspheres. Table I presents the atomic compositions determined from the XP spectra results. The changes in the atomic composition may have been due to the interfacial interaction between GO and the PS microspheres through the PANI nanofibers.

Figure 3 shows the Raman spectra of (a) pure PANI, (b) PANI-PS, (c) PANI-PS/GO composite, and (d) GO, as well as that of pure PS, for comparison. For the pure PS in Figure 3(a), the strong bands observed at 620, 790, 1010, 1187, and 1323 cm^{-1} were assigned to the aromatic rings of PS.[26] The strong peak at 1604 cm^{-1} was ascribed to the C=C frequency of styrene. The peaks at 3062 and 2900 cm^{-1} were assigned to the symmetric and antisymmetric CH_2 valence vibrations, respectively.[27] For the pure PANI (Figure 3(a)), a strong

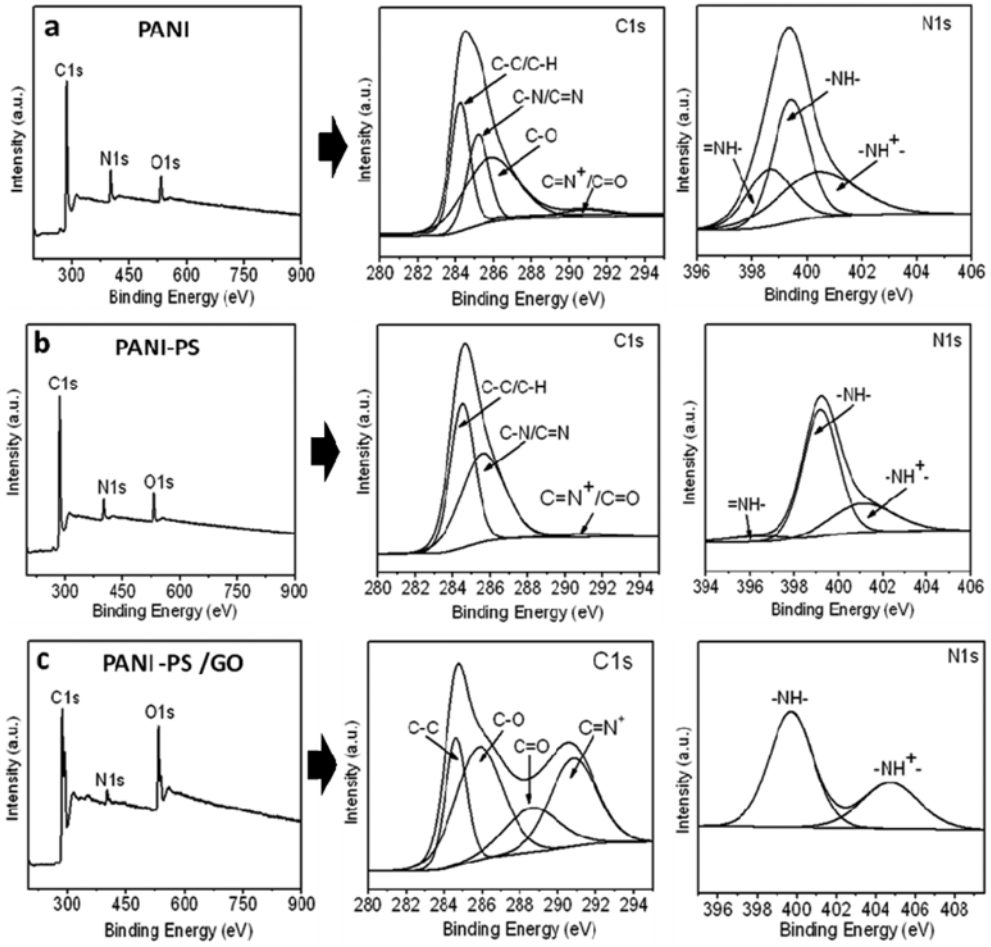

Figure 2. XPS data of (a) PANI, (b) PANI-PS, and (c) PANI-PS/GO core-shell composite.

Table I. XPS Atomic Composition of the Pure PANI, PANI-PS, and PANI-PS/GO Core-Shell Composites

Sample	Atomic Composition (%)		
	C	O	N
Pure PANI	78.58	7.9	10.66
PANI-PS	80.14	7.74	7.8
PANI-PS/GO Core-Shell Composite	82.11	14.83	2.97

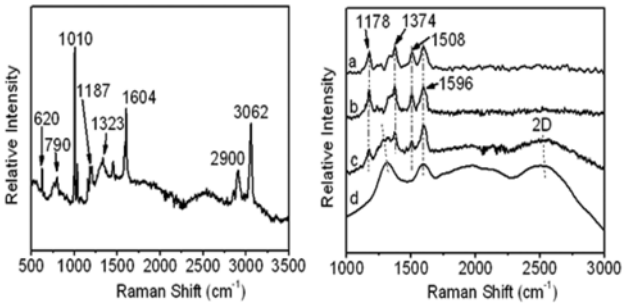

Figure 3. Raman spectra of pure PS (Right) and of (a) pure PANI, (b) PANI-PS, (c) PANI-PS/GO composite, and (d) GO (Left).

peak at 1178 cm^{-1}, corresponding to the C-H bending of the quinoid ring, C-N^+ stretching at 1374 cm^{-1} and C-C stretching of the quinoid and benzene rings at 1508 and 1596 cm^{-1}, respectively, were observed.[28] The peaks of the PANI-PS and PANI-PS/GO composites (seen in Figures 3(b) and 3(c)) were almost identical to those of pure PANI, indicating the existence of PANI on the surface of the PS microsphere. In addition, a new peak at 1285 (D- band) and 2570 cm^{-1} corresponding to the 2D band of GO,[29] indicate the successful interaction of the PANI-PS with GO.

Figure 4 shows the scanning electron microscopy (SEM) images of the pure PS and PANI-coated PS. For the pure PS in Figure 4(a), the smooth surface of the PS microsphere confirmed the successful polymerization of PS via suspension polymerization. The morphology of the PANI-coated PS (Figure 4(b) and (c)) at different magnifications demonstrated that the PS microspheres were uniformly and smoothly coated with PANI nanofibers, as shown in Figure 4(c). This good dispersion of PANI on the PS surface may have been due to the sulfonation process of PS to generate

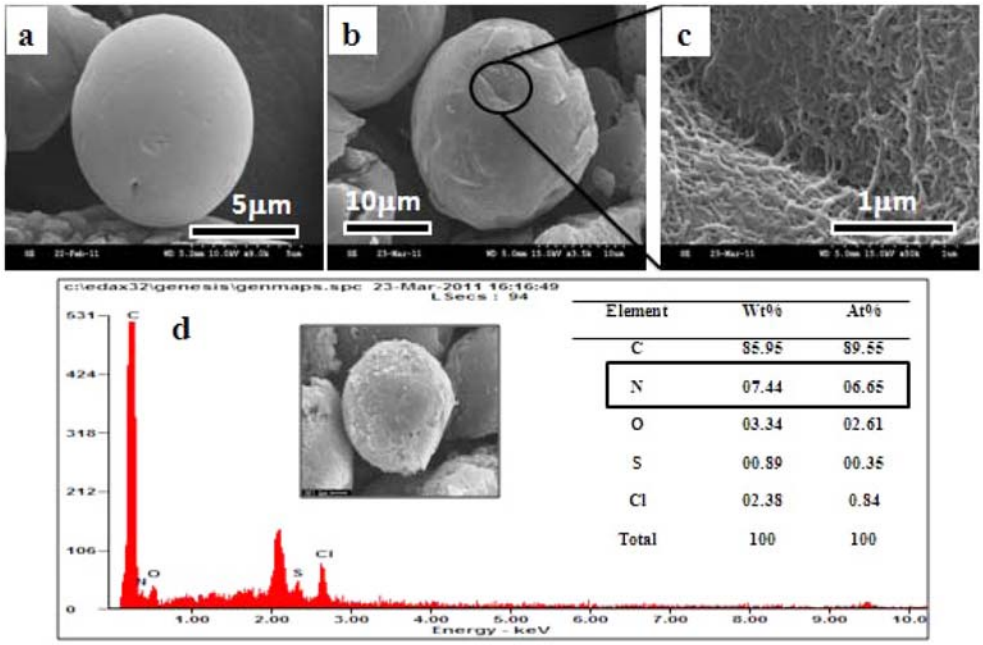

Figure 4. SEM images of (a) pure PS, (b) and (c) of PANI-PS at different magnifications, and (d) EDX images of PANI-PS.

sufficient sulfonic acid groups on the surface of the PS microspheres. The presence of PANI nanofibers on the PS surface was analyzed by energy-dispersive X-ray spectroscopy (EDX) with SEM. The EDX spectrum (Figure 4(d)) strongly shows the presence of a nitrogen peak, which confirmed the existence of PANI nanofibers on the surface of PS. This result was also confirmed by FTIR and Raman spectroscopy.

Figure 5 presents SEM images of the PANI-PS and PANI-PS/GO core-shell composites at different magnifications. PANI was well dispersed on the surface of PS (Figure 5(a) and (b)) without and agglomeration, which was attributed to the presence of sufficient sulfonic acid groups on the PS surface due to the enhancement of the interfacial interaction between the amine group of aniline and the sulfonic acid groups. This sulfonation PS and variation in the aniline concentration not only controlled the uniformity of the dispersion of PANI nanofibers on the PS surface but also offered a simple means of tuning the wall thickness.[30] Figure 5(c) shows the PANI nanofiber residues after THF extraction of the PS from PANI-coated PS. Because THF is a good solvent for PS but a poor one for PANI, a hollow structure made

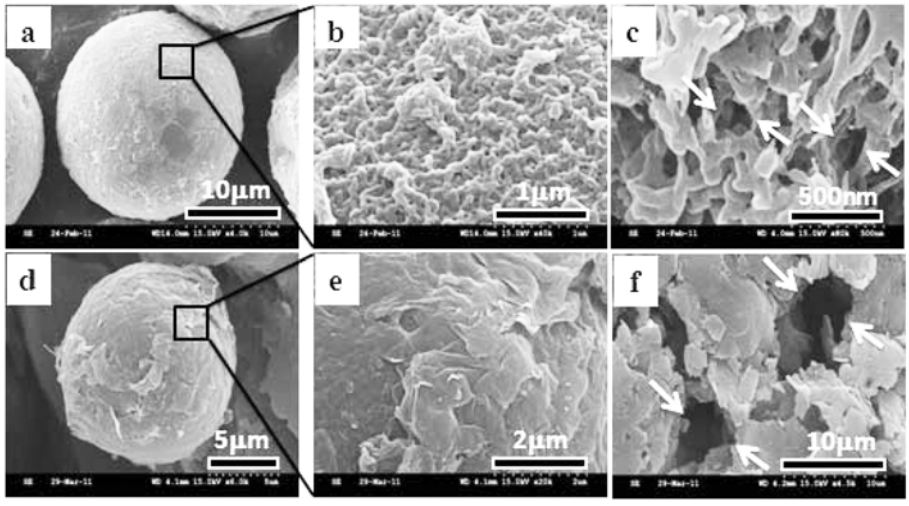

Figure 5. (a) and (b) SEM images of PANI-PS at different magnifications. (c) SEM image of PANI nanofiber residues after THF extraction of the PS from PANI-PS. (d) and (e) SEM images of PANI-PS/GO core-shell composite at different magnifications. (f) SEM image of the PANI/GO residues after THF extraction of the PS from PANI-PS/GO core-shell composite.

of these PANI residues could be obtained by selectively dissolving the PS microspheres in THF. This process was used to calculate the quantitative deposition of all PANI nanofibers on the surface of the PS microspheres after the elimination of PS. The images in Figure 5(d) and (e) of the PANI-PS/GO core-shell composite under different magnifications show the uniformly coated surface of the PANI-PS with GO sheets forming a core-shell structure through the ring opening reaction of the epoxide groups in the GO sheets with the amine groups in the PANI nanofibers. These good interfacial interactions provided a uniform dispersion of GO over the surface of the PANI-PS without aggregation, while exhibiting a similar average thickness of GO on the PS surface. These results confirmed the successful preparation of the PANI-PS/GO core-shell composite. In addition, the investigated morphology of the PANI/GO residues (Figure 5(f)) after THF extraction of PS from the PANI-PS/GO core-shell composite by SEM revealed a 'broken egg shell' morphology, which confirmed the 'core-shell' morphology of the original PANI-PS/GO composite. The diameter of the 'egg shell' decreased dramatically due to the total elimination of PS and the aggregation of GO sheets after THF extraction of the PS microspheres compared to the original morphology. This confirmed the existence of GO sheets on the surface of the PANI-coated PS. The morphology of the PANI-coated PS was examined by TEM to observe the individual structure and to estimate the coating thickness of PANI on the surface of PS microspheres.

Figure 6 shows TEM images of the PANI-PS and PANI-PS/GO core-shell microsphere composite. The TEM images in Figure 6(a), (b), and (c) correspond to the PANI-coated PS at different magnifications. The entire surface of the PS microsphere was coated with PANI. The coating thickness of PANI was estimated to be approximately 104 nm from the magnified image of the microsphere composite in Figure 6(c). The PANI-PS/GO core-shell microsphere composite shown in Figure 6(d), (e), and (f) shows that the GO sheets covered the entire surface of the PANI-coated PS without aggregation, and that PANI was almost invisible due to the complete covering by the GO sheets. This confirmed the strong interfacial interaction through a ring opening reaction of the epoxide groups in the GO sheets with amine groups in the PANI nanofibers. The coating thickness of the GO sheets on the surface of the PANI-PS was estimated as approximately 300 nm from the magnified picture of the core shell composite in Figure 6(f). To understand the effect of the PANI nanofibers and GO sheets on the thermal behaviors of the PANI-PS and PANI-PS/GO core-shell microsphere composite, DSC and TGA analysis were used to identify the thermal stability of the pure PS microspheres, PANI-PS and PANI-PS/GO core-shell microsphere composite.

Figure 7 shows the DSC heating curves of the pure PS microspheres, PANI-PS and PANI-PS/GO core-shell microsphere composite at a heating rate of 20 °C/min under a nitrogen atmosphere. From the DSC result, the T_g values of the PS microspheres and PANI-PS were 100.87 and 105.03 °C, respectively, as shown in Figure 7(b). This approximate 4 °C variation in T_g was possibly due to the action of the high-T_g PANI nanofibers dispersed on the surface of the PS cores as a thermal barrier that inhibited the mobility of the PS polymer chains during the DSC heating scans.[31] Ding reported that the T_g of pure PANI (base form) was approximately 250 °C[32] and Qi found that it was approximately 163.19 °C in the presence of HCl as a dopant.[33] This difference might be due to the different crosslinking degree of the PANI chains. For the PANI-PS/GO core-shell microsphere composite, T_g was shifted to 107.9 °C, showing an approximate 3 °C increase compared to the PANI-PS, as shown in Figure 7(c). The increase in T_g of the PANI-PS/GO core-shell microsphere composite may have been due to motion restrictions of the polymer chains at the interface of the PANI-PS and GO sheets.[34]

Figure 8 and Table II show the TGA results for the GO, pure PANI, neat PS, PANI-PS, and PANI-PS/GO composite

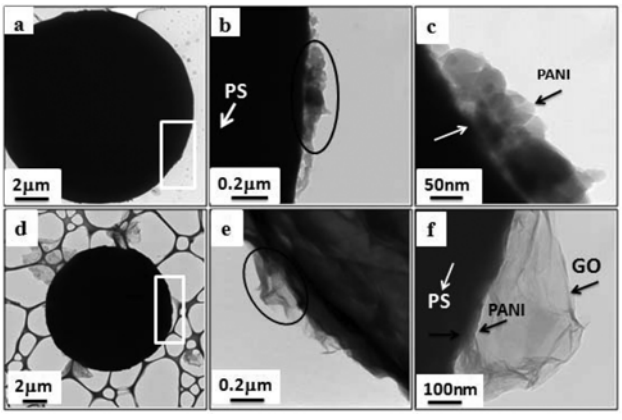

Figure 6. (a), (b), and (c) TEM images of PANI-PS at different magnifications. (d), (e), and (f) TEM images of PANI-PS/GO core-shell microsphere composite at different magnifications.

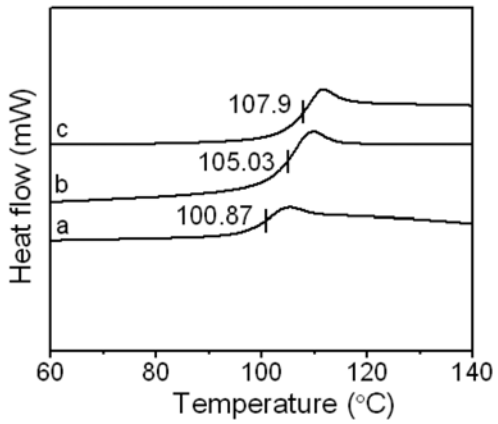

Figure 7. DSC of (a) neat PS, (b) PANI-PS, and (c) PANI-PS/GO core-shell microsphere composite.

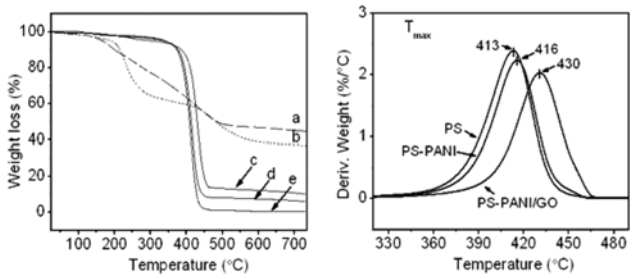

Figure 8. (Right) TGA of (a) GO, (b) pure PANI, (c) PANI-PS/GO, (d) PANI-PS, and (e) neat PS, and (Left) the *corresponding* weight loss derivative curve of PS, PANI-PS and PANI-PS/GO.

using nitrogen at a rate of 10 ºC/min. The GO weight-loss behavior in Figure 8(a) shows a dramatic mass loss of approximately 56% from ~100 to 730 ºC due to the decomposition of oxygen-containing groups.[35] A typical three-step weight-loss behavior was observed for the PANI nanofibers, as reported in the literature.[36] In the first step, from approximately 20 to 200 ºC, water molecules were lost from the polymer chain. The second weight loss in the range from 200-420 ºC was attributed to the loss of oligomers and dopants. The third weight loss above 420 ºC was caused by the degradation and decomposition of the PANI chain. The TGA data of neat PS, shown in Figure 8(e) for comparison, revealed that the thermal profile of the pure PS microspheres was a single-step weight loss. The main step of PS degradation was from 300 to 450 ºC, which was attributed to main chain pyrolysis,[37] beginning from 340 ºC with the evolution of aromatics from the degradation of styrene. For the PANI-PS shown in Figure 8(d), a similar weight-loss behavior of neat PS was observed from 25 to 350 ºC due to the good interfacial interaction between PS and PANI. The degradation of the PS microspheres in the PANI-PS was observed from 350 to 450 ºC. Furthermore, the degradation temperature of PS in the PANI-coated PS shifted to a higher temperature range than that of the neat PS, which suggests a strong interaction between the PANI and the PS microsphere at the interface. The PANI-PS/GO core-shell composite shown in Figure 8(c) exhibits two steps in the degradation of the composite. The first step from 200 to 350 ºC is due to the existence of water in the GO sheets as well as the degradation of GO. The second step, from ~350 to 460 ºC, was attributed to the degradation of the PANI-PS. Furthermore, the degradation temperature shifted to a higher temperature range than that of PANI-PS, which suggests a strong interaction between the amine groups in the PANI and the epoxide groups in the GO sheets at the interface.

For comparison, the TGA curves show that at 730 ºC, when there was almost no PS residue, the charred residue of the PANI from the PANI-PS was approximately 6.4%, after deducting the char yield of PANI, compared to 36.88% for neat PANI at the same temperature. The charred residue of the PANI/GO from the PANI-PS/GO core-shell composite was approximately 10.52%, after deducting the char yield of PANI/GO, compared to 45.02% for the neat GO at the same temperature. These results enabled the residue of GO from the charred residue of the PANI/GO at 730 ºC to be calculated by subtracting the charred residue of PANI from PANI-PS at 730 ºC, to obtain 4.12% of charred residue of GO at this temperature. These results suggested that the introduction of GO to PANI-PS enhanced the formation of char on the PS surface and, thus, reduced the rate of decomposition.

For more confirmation, the charred residue of PANI and PANI/GO at 730 ºC was examined by scanning electron microscopy (SEM), to confirm the total degradation of PS from the PANI-PS/GO core-shell composite, as shown in Figure 9. A hollow sphere of the charred residue of PANI, with a diameter of approximately 350 nm, was clearly obtained after the TGA measurement from the PANI-coated PS with some aggregation of PANI due to the degradation in some parts of the PANI structure, as shown in Figure 9(a). These results confirmed the total degradation of PS from the composite. The same observation was obtained for the charred residue of the PANI/GO from the PANI-PS/GO core-shell composite, as clearly shown in Figure 9(b). The degradation of PS from the composite led to the aggregation of GO layers with hollow spheres in some parts due to the total degradation of the PS microspheres, and the random dispersion of the charred residue of the PANI on the charred residue of GO. The charred residue of the PANI from the PANI-PS was confirmed by EDX. As shown in Figure 9(c), the EDX spectrum revealed the presence of a nitrogen peak with 7.62 wt%, which indicated the existence of the charred residue of the PANI from the PANI-PS. This confirmed the superior thermal stability of the PANI-PS and PANI-PS/GO compared to that of the neat PS microspheres during the thermal

Table II. Thermal Stability of the Neat PS, PANI-PS and PANI-PS/GO Core-Shell Composite

Sample	$T_{10\%}{}^{a}$ (°C)	$T_{50\%}{}^{a}$ (°C)	$T_{max}{}^{a}$ (°C)	$T_g{}^{b}$ (°C)	Char Yield[a] (%)
PS	372	407	411	100.87	0
PANI-PS	376	413	417	105.03	6.4
PANI-PS/GO	386	428	432	107.9	10.52

[a]Determined by TGA. [b]Determined by DSC. $T_{10\%}$ (ºC): thermal decomposition temperature at 10% weight loss. $T_{50\%}$ (ºC): thermal decomposition temperature at 50% weight loss. T_{max} (ºC): thermal decomposition temperature at the maximal weight loss rate, this T_{max} was calculated from the points with the steepest tangent slope or the peak value of the differential curve of the virgin curve as shown in Figure 7(b).

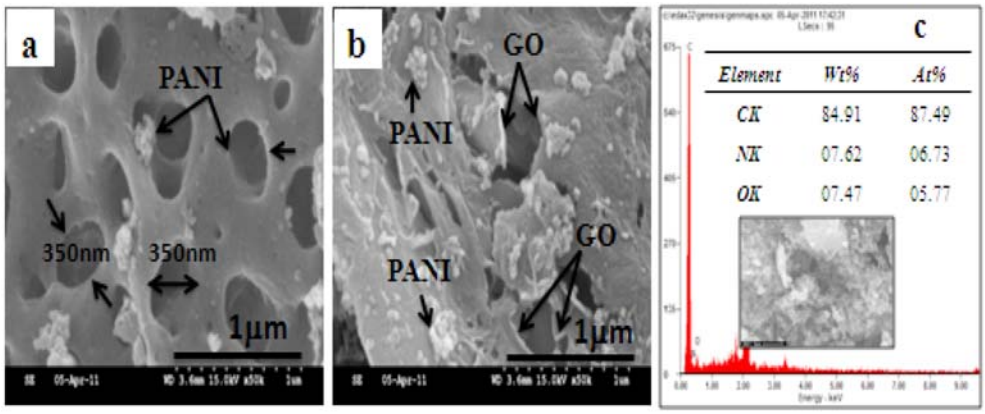

Figure 9. SEM images of (a) PANI-PS, and (b) PANI-PS/GO, and (c) EDX images of the PANI-PS composite after TGA analysis at 730 °C.

Table III. Mean Electrical Conductivities of the GO and Composites

Sample	Conductivity (S/cm)
GO	2.74×10^{-9}
PS	2.45×10^{-12}
PANI	1.05×10^{-4}
PANI-PS	1.32×10^{-6}
PANI-PS/GO	4.67×10^{-7}

decomposition process.

The electrical conductivity of the GO, PANI, PS, PANI-PS, and PANI-PS/GO composites was determined for pellets pressed from a powder using a four-probe resistivity measurement system. The average electrical conductivities are presented in Table III. The well ordered PANI nanofibers on the surface of the PS microspheres and the good interaction at the interface were key factors for enhancing the electrical conductivity of the PANI-PS composite. The incorporation of GO into the PANI-PS to form a PANI-PS/GO core-shell composite decreased the electrical conductivity due to the low conductivity of GO. The PANI-PS/GO composite showed relatively high electrical conductivity (4.67×10^{-7} S/cm) compared to that of GO (2.74×10^{-9} S/cm) due to the incorporation of PANI nanofibers into the PS/GO core-shell composite, which indicated that the incorporation of PANI nanofibers not only enhanced the interfacial interaction, but also improved the electrical conductivity of the final composite.

Conclusions

A simple method was developed to produce a PANI-PS/GO core-shell composite through a solution mixing process. The PS microspheres were well covered by GO sheets due to the presence of PANI nanofibers polymerized on the surface of the s-PS microspheres. This compositional structure ensured good interaction at the interface through the ring opening reaction of the epoxide groups in the GO sheets with the amine groups in the PANI nanofibers. The existence of PANI nanofibers was confirmed by FTIR, Raman spectroscopy and EDX. The PANI-PS/GO core-shell composite exhibited better thermal stability than did the neat PS microspheres. In addition, the electrical conductivity investigations revealed that the presence of PANI in the composite enhanced the interfacial interaction and improved the electrical conductivity of the composite. The increased electrical conductivity of the final composite may support potential electronics applications.

Acknowledgements. This study was supported by INHA UNIVERSITY Research Grant.

References

(1) K. R. Reddy, B. C. Sin, C. H. Yoo, D. Sohn, and Y. Lee, *J. Colloid Interface Sci.*, **340**, 160 (2009).
(2) A. K. Geim and K. S. Novoselov, *Nat. Mater.*, **6**, 183 (2007).
(3) S. Stankovich, D. A. Dikin, G. H. B. Dommett, K. M. Kohlhaas, E. J. Zimney, E. A. Stach, R. D. Piner, S. T. Nguyen, and R. S. Ruoff, *Nature,* **442**, 282 (2006).
(4) S. Stankovich, D. A. Dikin, R. D. Piner, K. A. Kohlhaas, A. Kleinhammes, Y. Jia, Y. Wu, S. T. Nguyen, and R. S. Ruoff, *Carbon,* **45**, 1558 (2007).
(5) W. S. Hummers and R. E. Jr. Offeman, *J. Am. Chem. Soc.*, **80**, 1339 (1958).
(6) H. He, T. Riedl, A. Lerf, and J. Klinowski, *J. Phys. Chem.*, **100**, 19954 (1996).
(7) C. Hontoria-Lucas, A. J. Lopez-Peinado, J. de D. Lopez-Gonzalez, M. L. Rojas-Cervantes, and R. M. Martiz-Randa, *Carbon*, **33**, 1585 (1995).
(8) Y. Si and E. T. Samulski, *Nano Lett.*, **8**, 1679 (2008).
(9) J. I. Paredes, S. Villar-Rodil, A. Martinez-Alonso, and J. M. D. Tascon, *Langmuir*, **24**, 10560 (2008).
(10) D. R. Dreyer, S. Park, C. W. Bielawski, and R. S. Ruoff, *Chem. Soc. Rev.*, **39**, 228 (2010).
(11) T. Wei, G. Luo, Z. Fan, C. Zheng, J. Yan, C. Yao, W. Li, and

C. Zhang, *Carbon*, **47**, 2290 (2009).
(12) Q. Bao, H. Zhang, J.-X. Yang, S. Wang, D.-Y. Tang, R. Jose, S. Ramakrishna, C.-T. Lim, and K.-P. Loh, *Adv. Funct. Mater.*, **20**, 782 (2010).
(13) J. Y. Jang, M. S. Kim, H. M. Jeong, and C. M. Shin, *Compos. Sci. Technol.*, **69**, 186 (2009).
(14) R. Ding, Y. Hu, Z. Gui, R. Zong, Z. Chen, and W. Fan, *Polym. Degrad. Stab.,* **81**, 473 (2003).
(15) W. L. Zhang, Y. D. Liu, and H. J. Choi, *J. Mater. Chem*., **21**, 6916 (2011).
(16) P. Guo, H. Song, and X. Chen, *J. Mater. Chem*., **20**, 4867 (2010).
(17) H. Hu, X. Wang, J. Wang, L. Wan, F. Liu, H. Zheng, R. Chen, and C. Xu, *Chem. Phys. Lett.,* **484**, 247 (2010).
(18) Y. Cao, J. Feng, and P. Wu, *Carbon*, **48**, 1670 (2010).
(19) M. A. Lopez-Manchado, B. Herrero, and M. Arroyo, *Polym. Int*., **53**, 1766 (2004).
(20) J.-H. Du, J. Bai, and H.-M. Cheng, *Express Polymer Lett.,* **1**, 253 (2007).
(21) Y. Yang, Y. Chu, F. Yang, and Y. Zhang, *Mater. Chem. Phys.*, **92**, 164 (2005).
(22) B. H. Sung, U. S. Choi, H. G. Jang, and Y. S. Park, *Colloids Surf. A: Physicochem. Eng. Asp.*, **274**, 37 (2006).
(23) S. Parveen, C. Veena, B. P. Singh, R. B. Mathur, and S. K. Dhawan, *Mater. Chem. Phys.,* **113**, 919 (2009).
(24) F. Yilmaz and Z. Kucukyavuz, *J. Appl. Polym. Sci.*, **111**, 680 (2009).
(25) G. X. Wang, B. Wang, J. Park, J. Yang, X. P. Shen, and J. N. Yao, *Carbon*, **47**, 68 (2009).
(26) A. Palm, *J. Phys. Chem*., **55**, 1320 (1951).
(27) E. J. C. Kellar, A. M. Evans, J. Knowles, C. Galiotis, and E. H. Andrews, *Macromolecules*, **30**, 2400 (1997).
(28) T.-M. Wu, Y.-W. Lin, and C.-S. Liao, *Carbon*, **43**, 734 (2005).
(29) A.-C. Ferrari, J.-C. Meyer, V. Scardaci, C. Casiraghi, M. Lazzeri, F. Mauri, S. Piscanec, D. Jiang, K.-S. Novoselov, S. Roth, and A.-K. Geim, *Phys. Rev. Lett*., **97**, 187401 (2006).
(30) M.-Y. Bai, Y.-J. Cheng, S. A. Wickline, and Y. Xia, *Small*, **5**, 1747 (2009).
(31) E.-C. Chen, Y.-W. Lin, and T.-M. Wu, *Polym. Degrad. Stab.,* **94**, 550 (2009).
(32) L. L. Ding, X. W. Wang, and R. V. Gregory, *Synth. Met*., **104**, 73 (1999).
(33) Y.-N. Qi, F. Xu, H.-J. Ma, L.-X. Sun, J. Zhang, and T. Jiang, *J. Therm. Anal. Calorim.*, **91**, 219 (2008).
(34) A. S. Patole, S. P. Patole, H. Kang, J.-B. Yoo, T.-H. Kim, and J.-H. Ahn, *J. Colloid Interface Sci.,* **350**, 530 (2010).
(35) M.-J. McAllister, J.-L. Li, D.-H. Adamson, H.-C. Schniepp, A-A. Abdala, J. Liu, M. Herrera-Alonso, D.-L. Milius, R. Car, R.-K. Prud'homme, and I.-A. Aksay, *Chem. Mater.*, **19**, 4396 (2007).
(36) S. Palaniappan and B. H. Narayana, *J. Polym. Sci. Part A: Polym. Chem.*, **32**, 2431 (1994).
(37) M. Suzuki and C. A. Wilkie, *Polym. Degrad. Stab*., **47**, 217 (1995).